

Millimeter Wave Massive MIMO Downlink Per-Group Communications with Hybrid Linear Precoding

T. Ketseoglou, *Senior Member, IEEE*, M.C. Valenti, *Fellow, IEEE*, and
E. Ayanoglu, *Fellow, IEEE*

Abstract

We address the problem of analyzing and classifying in groups the downlink channel environment in a millimeter-wavelength cell, accounting for path loss, multipath fading, and User Equipment (UE) blocking, by employing a hybrid propagation and multipath fading model, thus using accurate inter-group interference modeling. The base station (BS) employs a large Uniform Planar Array (UPA) to facilitate massive Multiple-Input, Multiple-Output (MIMO) communications with high efficiency. UEs are equipped with a single antenna and are distributed uniformly within the cell. The key problem is analyzing and defining groups toward precoding. Because equitable type of throughput is desired between groups, Combined Frequency and Spatial Division and Multiplexing (CFSDM) prevails as necessary. We show that by employing three subcarrier frequencies, the UEs can be efficiently separated into high throughput groups, with each group employing Virtual Channel Model Beams (VCMB) based inner precoding, followed by efficient Multi-User Multiple-Input Multiple-Output (MU-MIMO) outer precoders. For each group, we study three different sub-grouping methods offering different advantages. We show that the improvement offered by Zero-Forcing Per-Group Precoding (ZF-PGP) over Zero-Forcing Precoding (ZFP) is very high.

I. INTRODUCTION

Millimeter wave (mmWave) band communication is an attractive solution for future wireless applications, because it offers a wide spectrum that can support short-range high-rate wireless

T. Ketseoglou is with the Electrical and Computer Engineering Department, California State Polytechnic University, Pomona, USA (e-mail: tketseoglou@cpp.edu). M. Valenti is with the Lane Department of Computer Science and Electrical Engineering, West Virginia University, Morgantown, USA (email: mvalenti@wvu.edu). E. Ayanoglu is with the Electrical Engineering and Computer Science Department, University of California, Irvine, USA (e-mail: ayanoglu@uci.edu). This work was partially supported by NSF grant 1547155.

connectivity [1]. In addition, downlink input-output mutual information maximizing (IOMIM) linear precoding with finite-alphabet inputs, e.g., by employing Quadrature Amplitude Modulation (QAM), has been extensively studied [2]–[7] due to its potential to offer high data rate collectively. However, all existing analysis focuses on multipath fading without considering essential propagation effects in mmWave communications such as UE blocking, path loss, and varying fading scaling factors. The latter effects have been modeled in [8], [9] for mmWave device-to-device communications in a flexible way with success. In this paper, we apply the model proposed in [8], [9] for the cell interference effects and combine it with UE grouping techniques in order to analyze the potential of separating users in quasi-orthogonal groups in 5G mmWave bands, when the number of total UPA elements at the BS is large, i.e., in massive MIMO, in order to improve performance and simplify complexity. Furthermore, IOMIM linear precoding techniques tend to offer varying throughput to different UEs depending on their received signal-to-noise ratio (SNR), i.e., a varying quality-of-service (QoS) among UEs. Finally, group-forming techniques in conjunction with IOMIM such as Joint Spatial Division and Multiplexing for Finite Alphabets (JSDM-FA) [5] have not been studied with realistic assumptions, e.g., non-orthogonality between different groups. In this paper, we address all these open issues. We focus on applying CFSDM [5] techniques to divide UEs in groups in order to offer equalized QoS to all UEs in a cell. Furthermore, we apply different sub-grouping (SBG) forming techniques within each CFSDM subcarrier, in order to achieve high throughput with low complexity. These SBG techniques form the inner precoders of each group, based on the Virtual Channel Model Beams (VCMB) approach that was presented in [5], [10]. There are three techniques proposed and analyzed for SBG, including JSDM-FA together with a careful inter-sub-group interference analysis.

The contributions of this paper can be summarized as follows:

- 1) It employs a realistic mmWave communications model for the massive MIMO downlink within a cell, that includes random UE blocking, path loss, and multipath fading effects.
- 2) It presents a comprehensive approach to dividing UEs in groups based on their initial QoS, then subdivide groups in sub-groups by SBG in order to improve performance and lower the system complexity.
- 3) It presents results for three types of SBG, including detailed inter-sub-group interference analysis in the case of JSDM-FA
- 4) It shows that due to the debilitating impact of mmWave channels, the outer precoder in

each group faces high channel correlation that leads to very poor performance of ZFP.

- 5) It demonstrates that in general JSMD-FA suffers a performance loss over Total Grouping (TG) and Simple Grouping (SG), due to its inherent significant inter-sub-group interference (lack of orthogonality).
- 6) It shows very high gains of ZF-PGP over ZFP in performance over a wide range of SNR.

II. SYSTEM MODEL AND PROBLEM STATEMENT

A. MmWave Channel Model Employing Random UE Blocking, Path Loss, and Multipath Fading

We assume a dense population of UEs that are uniformly distributed within an annular cell of interior radius r_i and exterior radius r_o [9]. The BS UPA has height h and employs an x (horizontal), z (vertical) orientation. The total population of UE in the cell is N_{UE} . Each UE employs a single, uniformly radiating antenna. By employing Time Division Duplexing (TDD), the downlink channels will be reciprocal to the uplink ones. The uplink channel between UE n ($1 \leq n \leq N_{UE}$) is denoted by \mathbf{h}_n . With $P = 1$ multipath components [5], due to mmWave conditions, we get

$$\mathbf{h}_n = c_n (\mathbf{a}_z(\theta_n) \otimes \mathbf{a}_x(\theta_n, \phi_n)), \quad (1)$$

where \otimes denotes Kronecker matrix product, $c_n = |c_n| \exp(j2\pi b_n)$ is the multipath fading complex coefficient of amplitude $a_n = |c_n|$ and phase b_n , uniformly distributed in $[0, 2\pi]$, and θ_n, ϕ_n represent UE n 's ($1 \leq n \leq N_{UE}$) elevation and azimuth angle, respectively, and

$$\begin{aligned} \mathbf{a}_x(\theta_n, \phi_n) &= [1, \exp(-j2\pi D \sin(\theta_n) \cos(\phi_n)), \dots, \\ &\quad \exp(-j2\pi D(N_{u,y} - 1) \sin(\theta_n) \cos(\phi_n))]^T, \\ \mathbf{a}_z(\theta_n) &= [1, \exp(-j2\pi D \cos(\theta_n)), \dots, \\ &\quad \exp(-j2\pi D(N_{u,x} - 1) \cos(\theta_n))]^T, \end{aligned} \quad (2)$$

with $D = \frac{d}{\lambda}$, d being the distance between adjacent antenna elements, λ the wavelength, and $N_{u,x}, N_{u,y}$ representing the number of elements of the UPA in the x and y direction, respectively. The instantaneous received SNR at UE n ($1 \leq n \leq N_{UE}$) is

$$\text{SNR}_n = a_n^2 \frac{\text{SNR}_0}{R_n^k}, \quad (3)$$

where R_n represents the distance between the UPA and the UE, SNR_0 is the SNR at $R_n = r_i$, k is the path-loss exponent, and a_n^2 is the power gain of the fading. As in [8], [9], if UE n

($1 \leq n \leq N_{UE}$) is blocked, we call it non-line-of-sight (NLOS) and we use $k = 4$ and a_n is Nakagami with $m = 2$, while when the UE is not blocked, we call it line-of-sight (LOS) and we apply $k = 2$ and $m = 4$.

B. Problem Statement

From [10], an equivalent cell downlink channel receiving equation, after normalization and encompassing both large-scale and scale-scale effects [11], i.e., propagation loss, multipath fading, respectively, and noise effects (including Additive White Gaussian noise (AWGN) and Multiple-Access Interference (MAI)) can be written in the virtual domain¹ [5], [10] as follows

$$\mathbf{y}_d = \mathbf{H}_{u,v}^H \mathbf{G} \mathbf{x}_d + \mathbf{n}_{d,AWGN} + \mathbf{n}_{d,MAI} \quad (4)$$

where \mathbf{y}_d is the downlink received vector over all users and antennas of size $N_{UE} \times 1$, \mathbf{G} is the linear precoding matrix of size $N_T \times N_{UE}$, \mathbf{x}_d is the $N_{UE} \times 1$ vector of transmitted symbols² drawn independently from a QAM constellation, the downlink virtual channel matrix $\mathbf{H}_{v,d} = \mathbf{H}_{u,v}^H$, with $\mathbf{H}_{u,v}$ being the $N_T \times N_{UE}$ uplink virtual channel matrix from all N_{UE} users, employing N_T receiving antennas at the BS, E_s is the transmitted energy per symbol and \mathbf{n}_d represents the complex circularly symmetric Gaussian noise of mean zero and variance per component $\sigma_d^2 = 1$ (after normalization). We focus on the input-output mutual information $I(\mathbf{x}_d; \mathbf{y}_d)$ maximizing downlink precoding problem, where we assume that the channel is known at both the transmitter and the receiver(s)³, can now be cast as

$$\begin{aligned} & \underset{\mathbf{G}}{\text{maximize}} \quad I(\mathbf{x}_d; \mathbf{y}_d) \\ & \text{subject to} \quad \text{tr}(\mathbf{G} \mathbf{G}^H) = N_{UE}, \end{aligned} \quad (5)$$

where the constraint is due to keeping the total power transmitted from the BS to all downlink users with precoding equal to the one without precoding, after normalization of the AWGN has taken place. It is well-known that this problem is complexity-burdened and thus grouping

¹This is the channel representation in the VCM basis, also called in the literature the beam-domain representation.

²We assume that there is one symbol per receiving antenna in (4), for simplicity.

³In [10] we show that estimated channels can be used successfully instead of the perfect channel knowledge assumed here.

UEs offers a solution to this [10], [12]–[14]. However, in this paper we aim at offering equitable throughput to UEs, thus additional counter measures are needed to achieve this goal, as described below.

C. UE Grouping and Sub-grouping

a) Pre-selection (PS) of VCMBs

By projecting the uplink UPA response vector to the complete orthonormal basis $\mathbf{B}_{VCM} = (\mathbf{F}_{N_{u,z}} \otimes \mathbf{F}_{N_{u,x}})$ where \mathbf{F}_N represents the Discrete Fourier Transform (DFT) matrix of size N , [5] showed that with a large number of array elements, $N_T = N_{u,x}N_{u,z}$, e.g., $N_T \sim 100$ and with equal elements per dimension ($N_{u,x} = N_{u,z}$) this projection achieves a sparse representation of the UE channels with only a few components from the columns of $\mathbf{B} = (\mathbf{F}_{N_{u,z}} \otimes \mathbf{F}_{N_{u,x}})$ needed. Since only a few columns of the fully orthonormal matrix $(\mathbf{F}_{N_{u,z}} \otimes \mathbf{F}_{N_{u,x}})$ are needed to characterize each channel, these are called Virtual Channel Model Beams (VCMB). Furthermore, for spatially distant UEs, different users form quasi-orthogonal groups of non-intersecting VCMBs. In addition, VCMBs can be used to derive many useful spatial-domain features for the entirety of downlink channels in the cell. Here, we use the VCMB in the cell in a dimension-reduction way. First, we extract the most “loaded” VCMBs in the cell, by determining the $N_{V,INIT}$ VCMBs that carry the most instantaneous power to UEs. The parameter $N_{V,INIT}$ is determined by the percentage of overall power in the cell we aim at capturing. Due to the nature of the VCMB structure, only a fraction of the total N_T VCMBs are needed to guarantee that more than, e.g., 90%, of the total power is captured. This VCMB selection phase is called pre-selection (PS). The pseudo code for the PS algorithm is shown below in Algorithm 1.

b) CFSDM-based Grouping for Balanced QoS

In mmWave communications, the existence of NLOS UEs which suffer a significant additional propagation power loss requires placing all NLOS UEs in a separate frequency sub-carrier, then employing a higher level of power to improve the NLOS UE throughput, thus achieving equalized throughput with the LOS UEs. Furthermore, due to high spatial correlation of UE channels, some UEs, although in the LOS class, will also experience low QoS. This QoS imbalance can be mitigated by adding another separate sub-carrier to accommodate these UEs, thus offering a solution toward equalizing the cell QoS. Thus, by employing a total of three subcarriers in the form of CFSDM [5] in the cell, we can achieve equitable QoS. Thus, we will have three

CFSDM groups in the cell, G_1 is the LOS uncorrelated group, G_2 is the LOS high-correlated group, and G_3 is the NLOS group. The corresponding number of UEs in each CFSDM group is denoted by N_{g_1} , N_{g_2} , and N_{g_3} , respectively.

c) SBG Techniques

After CFSDM grouping UEs, there is additional space for further SBG for improved performance or lower complexity. It is important to mention that sub-grouping employs the same frequency for all subgroups in a group, i.e., spatial multiplexing takes place towards improved performance in each group. After PS takes place, in the reduced dimension VCMB space comprising $N_{V,INIT}$ VCMBs, there are many alternatives one can use for further SG different UEs in a group. In this paper we consider the following three:

- 1) Employ all pre-selected VCMBs in a group, abbreviated as TG.
- 2) Select only the strongest VCMBs in the group, abbreviated as SG, resulting in a final number of VCMBs per group, $N_{V,FINAL} = N_{g_i}$, $i = 1, 2, 3$, which equals N_{g_i} , which is significantly smaller than $N_{V,INIT}$.
- 3) JSMD-FA for semi-orthogonal sub-groups [5], [10], which offers $N_{V,FINAL}$ even smaller than SG, but in general it suffers intra-sub-group interference.

Algorithm 1 PS algorithm

- 1: **for** $i = 1$ to N_T **do**
 - 2: calculate power of VCMB i , $P_i = ||H_{u,v}[:, i]||^2$;
 - 3: **end for**
 - 4: sort in descending order the vector $\mathbf{P} = [P_1 \ P_2 \ \dots \ P_{N_T}]$, resulting in a new sorted power list vector $\mathbf{P}_s = [P_{s_1} \ P_{s_2} \ \dots \ P_{s_{N_{V,INIT}}}]$ and sorted VCMB list vector \mathbf{v}_s
 - 5: select the first $N_{V,INIT}$ entries of \mathbf{P}_s , \mathbf{v}_s and denote them \mathbf{P}_{PS} , \mathbf{v}_{PS} , respectively and calculate the total power in \mathbf{P}_{PS} as percentage of the original total power, i.e.,

$$P_F = \frac{\sum_{i=1}^{N_{V,INIT}} P_{s_i}}{\sum_{i=1}^{N_T} P_i};$$
 - 6: re-arrange the selected \mathbf{v}_{PS} VCMBs per UE in descending channel power order, resulting in a $N_{UE} \times N_{V,INIT}$ matrix $\mathbf{M}_{V,PS}$ used in further processing
-

e) Efficient MU-MIMO Outer Precoding

After groups and subgroups are selected and the pre-beamformer (inner precoder) is constructed, an MU-MIMO linear precoder (outer precoder) is deployed to offer individual and high data rate streams to each UE in a subgroup. References [12], [15] envisaged this type of hybrid precoding in order to achieve high throughput to each user in a group by employing a Zero-

Forcing Precoder (ZFP). However, since all the UEs in a formed group possess spatial similarity, the channels within a group are highly correlated. Thus, ZFP results in low data rates and low spectral efficiency. Here we apply a ZF-PGP [10] which combines the benefits of ZFP and Per-Group Precoding within Groups (PGP-WG) (Fig. 1) [16] in order to improve the performance. ZF-PGP also employs the Virtual Additional Antenna Concept (VAAC) in [10] that delivers two symbols to each UE, thus doubling the high SNR throughput of ZF-PGP over ZFP.

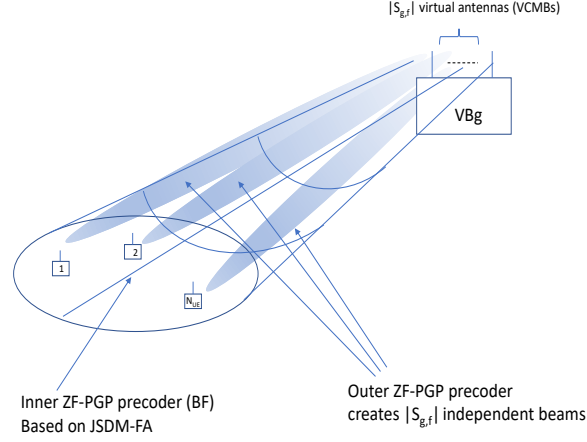


Fig. 1. Outer group precoder. After inner precoding, the outer ZF-PGP linear precoder creates $S_{g,f}$ independent data streams, one for each UE. $S_{g,f}$ denotes the final number of VCMBs in the sub-group.

III. NUMERICAL RESULTS

We present our numerical results for two cases: a) $N_{UE} = 10$, $r_i = 1$ m, $r_0 = 5$ m, and b) $N_{UE} = 20$, $r_i = 1$ m, $r_0 = 10$ m. For both cases, we consider multiple scenarios, including Total Grouping ZF-PGP (TGZF-PGP), Subgroup ZF-PGP (SGZF-PGP), and JSDM-FA ZF-PGP, and corresponding results for Zero-Forcing Precoding (ZFP). In order to offer high QoS to the NLOS UEs, we employ CFSDM [5], so that the LOS UEs employ a different subcarrier frequency than the NLOS ones. Furthermore, the NLOS UEs employ 13 dB higher power at the BS than the LOS UEs, in order to equalize the QoS in the NLOS group to the LOS groups one. Transmitted symbols are drawn from an $M = 16$ QAM constellation with two LOS groups selected from the S_{EFF} matrix of the virtual LOS channel, after the pre-selection VCMB phase. We use the (SNR) at distance $r_i = 1$ m from the BS array, as the horizontal variable in the figures.

For the $N_{UE} = 10$, $r_i = 1$ m, $r_0 = 5$ m cell deployment with TG and $N_{V,INIT} = 20$ (98 % of total cell power captured), we get 2 NLOS users, 5 UEs in G_1 , and 3 UEs in G_2 with results

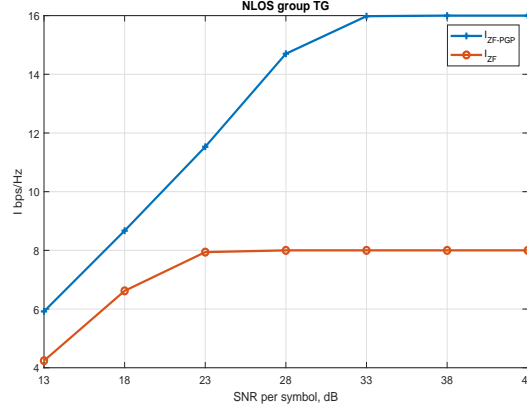


Fig. 2. Results for NLOS Group G_3 for the first deployment scenario.

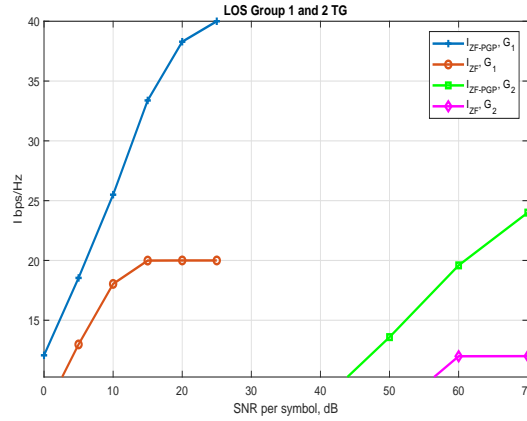


Fig. 3. Results for LOS Groups G_1 , G_2 for the first deployment scenario and TG.

depicted in Fig. 2. We observe that due to employing CFSDM with higher power, the NLOS group is able to attain high throughput. Applying TG to G_1 , G_2 , with $N_{V,INIT} = 20$, we get the results shown in Fig. 3. We observe that due to its high correlation channel, G_2 attains very low performance in comparison with G_1 .

In Fig. 4 we show results for G_2 with TG and SG. We observe that due to SG, the performance of G_2 is improved dramatically. We also notice that ZFP has come much closer to ZF-PGP, due to the SG approach.

For the $N_{UE} = 20$, $r_i = 1$ m, $r_0 = 10$ m cell deployment with TG and $N_{V,INIT} = 20$ (90 % of total cell power captured), we get the deployment of UEs showing in Fig. 5. For G_1 , G_2 with TG, we get the results shown in Fig. 6. We observe the same behavior as in the first deployment scenario, i.e., G_2 has significantly lower performance than G_1 , due to its

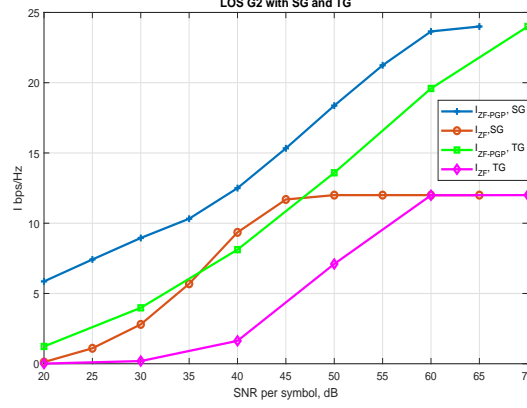


Fig. 4. Results for LOS Group G_2 for the first deployment scenario with SG and TG.

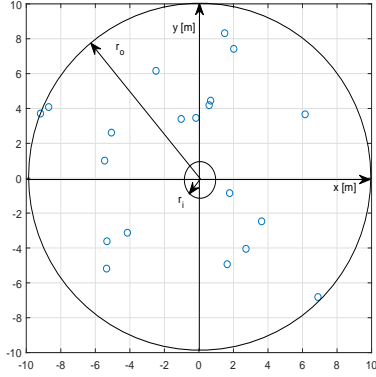


Fig. 5. Deployment of UEs for the $N_{UE} = 20$, $r_i = 1$ m, $r_0 = 10$ m scenario.

high correlation channel. For G_1 , G_2 with SG, we get the results shown in Fig. 7, showing a dramatic improvement to the performance of G_2 , however G_1 depicts a loss compared with TG. Finally, for JSDM-FA, we present numerical results for $N_{UE} = 10$, $r_i = 1$ m, $r_0 = 5$ m, by using a throughput lower bounding technique. After the VCMB pre-selection phase, there are $N_{V,INIT} = 20$ VCMBs employed in the cell which after PS result in selecting two subgroups in G_1 , denoted as G_{11} , G_{12} , respectively. The selection of UEs in the sub-groups is based on sharing the first few strongest VCMBs. This process results in the following sub-groups: G_{11} comprises rows $\{1, 2, 3\}$ of G_1 virtual channel, with VCMB numbers (after pre-selection) $\{7, 8, 12\}$, G_{12} comprises rows $\{5, 7\}$ of G_1 virtual channel, with corresponding VCMB numbers $\{21, 24\}$. A careful interference analysis, which is omitted here, reveals that there is $P_{IF} = 0.529$ normalized interfering power to G_{12} from G_{11} , while G_{12} is interference-free. In Fig. 8 we show

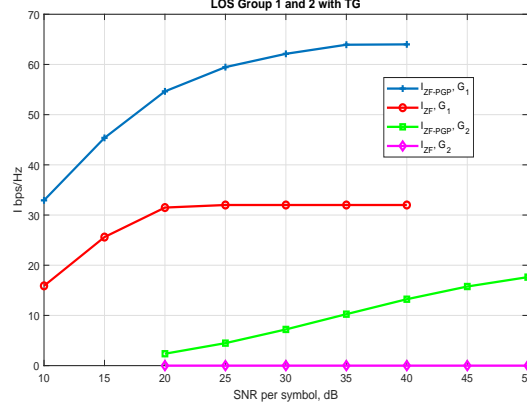


Fig. 6. Results for LOS Groups G_1 , G_2 for the second deployment scenario with TG.

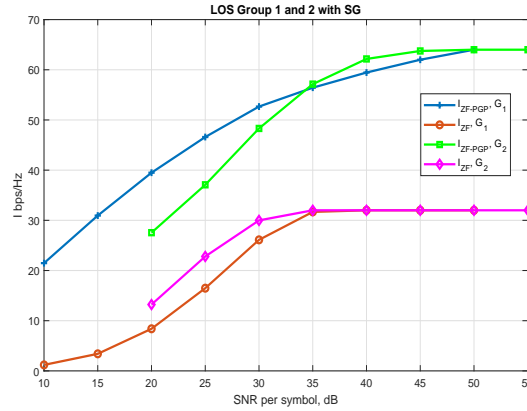


Fig. 7. Results for LOS Groups G_1 , G_2 for the second deployment scenario with SG.

the corresponding mutual-information results.

IV. CONCLUSIONS

We have applied the concept of ZF-PGP in a millimeter Wave massive cell, carefully modeling all channel intricacies, including UE blocking, path propagation, and multipath fading. It is shown that VCMBs offer many advantages in simplifying the channel representation, analyzing the system, and improving group and UE throughput. For the scenarios presented, it is shown that ZF-PGP offers significant throughput improvements, especially when the channel presents a high degree of correlation. When high correlation is present, ZF-PGP offers a 100% improvement in throughput over ZFP. When even higher correlation is present, ZF-PGP can offer more than 300% throughput improvement over ZFP, albeit in the lower SNR region. We compare three

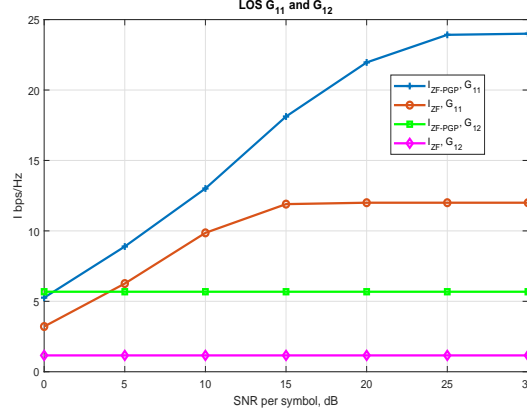


Fig. 8. Results for LOS Group G_1 for the second deployment scenario with JSDM-FA.

different VCMB-based group-forming techniques which offer different advantages, depending on the application scenario. Finally, our work has demonstrated that when $N_{UE} < 30$, only three subcarrier frequencies suffice for CFSDM to be used in the cell, in order to guarantee equitable QoS for all UEs. Our future work will also look at the impact of the array orientation, e.g., vertical, versus horizontal, together with a more accurate approximation to JSDM-FA performance.

REFERENCES

- [1] C. Park and T. S. Rappaport, "Short-Range Wireless Communications for Next-Generation Networks: UWB, 60 GHz Millimeter-Wave WPAN, and ZigBee," *IEEE Wireless Communications*, vol. 14, no. 4, pp. 70–78, August 2007.
- [2] T. Ketseoglou and E. Ayanoglu, "Linear Precoding Gain for Large MIMO Configurations with QAM and Reduced Complexity," *IEEE Transactions on Communications*, vol. 64, pp. 4196–4208, October 2016.
- [3] S. Zarei, W. Gerstacker, and R. Schober, "Robust MSE-Balancing Hierarchical Linear/Tomlinson-Harashima Precoding for Downlink Massive MU-MIMO Systems," *IEEE Transactions on Wireless Communications*, to appear.
- [4] C. Xiao, Y. Zheng, and Z. Ding, "Globally Optimal Linear Precoders for Finite Alphabet Signals Over Complex Vector Gaussian Channels," *IEEE Transactions on Signal Processing*, vol. 59, pp. 3301–3314, July 2011.
- [5] T. Ketseoglou and E. Ayanoglu, "Downlink Precoding for Massive MIMO Systems Exploiting Virtual Channel Model Sparsity," *IEEE Transactions on Communications*, vol. 66, pp. 1925–1939, May 2018.
- [6] Y. Wu, C.-K. Wen, D. Wing Kwan Ng, R. Schober, and A. Lozano, "Low-Complexity MIMO Precoding for Finite-Alphabet Signals," *IEEE Transactions on Wireless Communications*, vol. 16, no. 7, pp. 4571–4584, July 2017.
- [7] Y. Wu, C. Xiao, Z. Ding, X. Gao, and S. Jin, "A Survey on MIMO Transmission With Finite Input Signals: Technical Challenges, Advances, and Future Trends," *Proceedings of the IEEE*, vol. 106, no. 10, pp. 1779–1833, Oct 2018.
- [8] K. Venugopal, M. C. Valenti, and R. W. Heath, "Device-to-Device Millimeter Wave Communications: Interference, Coverage, Rate, and Finite Topologies," *IEEE Transactions on Wireless Communications*, vol. 15, no. 9, pp. 6175–6188, Sep. 2016.

- [9] E. Hriba, M. C. Valenti, K. Venugopal, and R. W. Heath, "Accurately Accounting for Random Blockage in Device-to-Device mmWave Networks," in *GLOBECOM 2017*, Dec 2017, pp. 1–6.
- [10] T. Ketseoglou and E. Ayanoglu, "Zero-Forcing Per-Group Precoding (ZF-PGP) for Robust Optimized Downlink Massive MIMO Performance," *IEEE Transactions on Communications*, vol. 67, no. 10, pp. 6816–6828, 2019.
- [11] A. Molisch, *Wireless Communications*. New York: Wiley-IEEE Press, 2011.
- [12] A. Adhikary, J. Nam, J. Y. Ahn, and G. Caire, "Joint Spatial Division and Multiplexing: The Large-Scale Array Regime," *IEEE Trans. Inf. Theory*, vol. 59, pp. 6441–6463, October 2013.
- [13] J. Nam, A. Adhikary, J. Y. Ahn, and G. Caire, "Joint Spatial Division and Multiplexing: Opportunistic Beamforming, User Grouping and Simplified Downlink Scheduling," *IEEE Journal of Selected Topics in Signal Processing*, vol. 8, no. 5, pp. 876–890, October 2014.
- [14] A. A. Nasir, H. D. Tuan, T. Q. Duong, and H. V. Poor, "Secure and Energy-Efficient Beamforming for Simultaneous Information and Energy Transfer," *IEEE Transactions on Wireless Communications*, vol. 16, no. 11, pp. 7523–7537, Nov 2017.
- [15] A. Adhikary, E. Al Safadi, M. K. Samimi, R. Wang, G. Caire, T. S. Rappaport, and A. F. Molisch, "Joint Spatial Division and Multiplexing for mm-Wave Channels," *IEEE Journal on Selected Areas in Communications*, vol. 32, no. 6, pp. 1239–1255, June 2014.
- [16] T. Ketseoglou and E. Ayanoglu, "Linear Precoding for MIMO with LDPC Coding and Reduced Complexity," *IEEE Transactions on Wireless Communications*, pp. 2192–2204, April 2015.